Supporting Information:

In Situ Synthesis of Morphology-Controlled MoO$_x$/Fe$_{1-x}$S Bifunctional Catalysts for High-Efficiency and Stable Alkaline Water Splitting

Ying Liu [a, c#], Xujiao Gu [a, c], Wei Jiang [a, d], Hongji Li [a, d], Yunchao Ma [a, c], Chunbo Liu [a,d]*,

Yuanyuan Wu [a, c]*, Guangbo Che [a,b]*

[a] *Key Laboratory of Preparation Application of Environmental Friendly Materials, Ministry of Education, Jilin Normal University, Siping 136000, P. R. China*

[b] *College of Chemistry, Baicheng Normal University, Baicheng 137000, P. R. China*

[c] *College of Chemistry, Jilin Normal University, Siping 13600, P. R. China*

[d] *College of Environmental Science and Engineering, Jilin Normal University, Changchun 130103, P. R. China*

[*] Corresponding author:

Chunbo Liu (chunboliu@jlnu.edu.cn); Yuanyuan Wu (yywu16@163.com); Guangbo Che (guangboche@jlnu.edu.cn),

Experimental Section

Chemicals and Reagents

All chemicals were of reagent grade and used without further purifications. Pt/C, IrO_2, Pluronic triblock copolymers P123, Thioacetamide (C_2H_5NS, TAA), Ammonium molybdate (($NH_4)_6Mo_7O_{24} \cdot 4H_2O$) were purchased from Aladdin (Shanghai, China). Fe foam (thickness: 1.5 mm) was purchased from Qinghe County Saiwei Metal Material Co., Ltd. Potassium hydroxide (KOH) and HCl were purchased from Beijing Chemical Factory. Highly purified water (>18 MΩ cm resistivity) was provided by a PALL PURELAB Plus system.

Synthesis of $MoO_x/Fe_{1-x}S/IF$ and $MoO_x/Fe_{1-x}S/IF-1$:

A piece of Fe foam (6 cm × 0.6 cm) was sonicated in 1 M HCl for 10 min to remove impurities and oxide layer on the surface. And then rinsed with anhydrous ethanol and deionized water three times each to remove any additional HCl, then left dry in the air. Ammonium molybdate (40 mg), thioacetamide (90 mg) and P123 (0.2 g) were dissolved in 60 mL of deionized water. The reaction mixture was stirred magnetically for 30 min at room temperature. The precursor solution was transferred into a 100 mL Teflon lined stainless steel autoclave loaded with a piece of Fe foam. The autoclave was sealed and maintained at 120 °C for 12 h, followed by cooling naturally (labeled as $MoO_x/Fe_{1-x}S/IF$). The synthesis method of $MoOx/Fe_{1-x}S/IF-1$ was similar to that of $MoOx/Fe_{1-x}S/IF$, except for the absence of P123 (labeled as $MoO_x/Fe_{1-x}S/IF-1$).

Synthesis of $Fe_{1-x}S/IF$ and $Fe_{1-x}S/IF-1$:

In order to determine the role of MoO_x on the catalytic activity of $MoO_x/Fe_{1-x}S/IF$, another $Fe_{1-x}S$ material supported on IF (denoted $Fe_{1-x}S/IF$) was prepared. Except for the amount of ammonium molybdate, the reagents and procedures used to make both materials were similar with those employed to make $MoO_x/Fe_{1-x}S/IF$. The synthesis method of $Fe_{1-x}S/IF-1$ was similar to that of $Fe_{1-x}S/IF$, except for the absence of P123 (labeled as $Fe_{1-x}S/IF-1$).

Characterization and Instrumentations:

The obtained products were examined by XRD (Thermo Fisher/Equinox 100 X-ray diffractometer with Cu Kα radiation (λ = 1.5418 Å)) at 2θ range of 20° to 80° with the scan speed of 10° min^{-1}. Raman spectra were collected with a Renishaw 2000 System. X-ray photoelectron spectroscopy (XPS) was tested on ESCALAB 250Xi X-ray photoelectron spectrometer with a monochromatic X-ray source (Al Kα hυ = 1486.6 eV). The morphology and microstructure of as-prepared products were conducted via scanning electron microscope (SEM, Regulus 8100) and transmission electron microscope (TEM, Philips-FEI Tecnai G_2S-Twin microscope).

Electrochemical Characterization:

All electrochemical tests were measured in 1 M KOH electrolyte using a traditional three-electrode setup by a CHI760E electrochemical workstation at room temperature, in which, Hg/HgO was served as the reference electrode, carbon rod as counter electrode, and the as-prepared electrodes as the working electrode. Linear sweep voltammetry (LSV) data was measured with a scan rate of 1 mV s $^{-1}$. In order to prepare Pt/C and RuO_2 working electrode, the powder Pt/C and RuO_2 was dissolved and dropped on the iron foam and dried naturally. The load mass was 0.3 mg cm^{-2}. The working electrode area was 0.09 cm^2, which was the same as as-prepared working electrodes. 5 μL isopropanol solution containing 0.3% Nafion was dropped on the sample to form a protective film to prevent the sample from falling off. Electrochemical impedance spectroscopy (EIS) was carried out from 100 kHz to 0.1 Hz at an overpotential of 300 mV. The overall water splitting performances were performed in a two electrode system, and the prepared $MoO_x/Fe_{1-x}S/IF-$

1 samples were worked as cathode and anode, respectively.

To determine the electrochemical active surface area (ECSA) of different samples, a series of CV curves were collected at different scan rates (20 to 90 mV s^{-1}) within an appropriate potential range (0.1 V-0.2 V) where no Faradaic reaction occurred. It could be found that the relationship of the double layer current and the scan rates could be linearly fitted. The slope of this linear fitting equation was the double-layer capacitance (C_{dl}). The ECSA was estimated to be:

$$ECSA=C_{dl}/C_s \times ASA,$$

Where C_s is the specific capacitance with a value of 0.04 mF cm^{-2} in this work, and ASA is the actual surface area of the electrode.
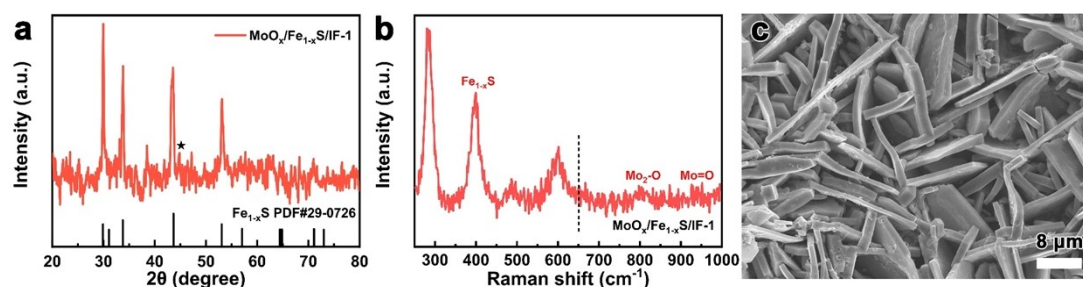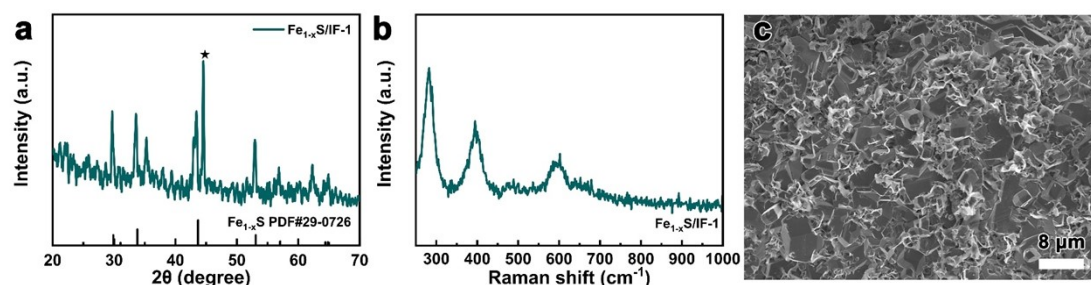

Figure S1. XRD pattern, Raman spectrum and SEM image of a material obtained from a control experiment. (a-c) P123 was not involved in the reaction system, but the other reaction parameters were kept unchanged.
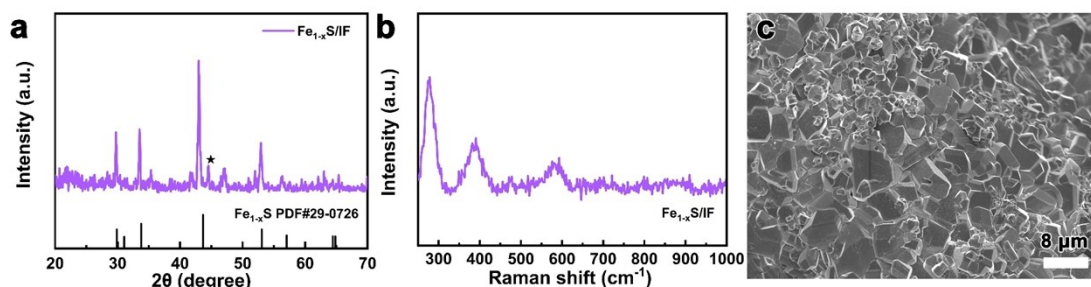
Figure S2. XRD pattern, Raman spectrum and SEM image of a material obtained from a control experiment. (a-c) Ammonium molybdate was not involved in the reaction system, but the other reaction parameters were kept unchanged.

Figure S3. XRD pattern, Raman spectrum and SEM image of a material obtained from a control experiment. (a-c) P123 and ammonium molybdate were not involved in the reaction system, but the other reaction parameters were kept unchanged.
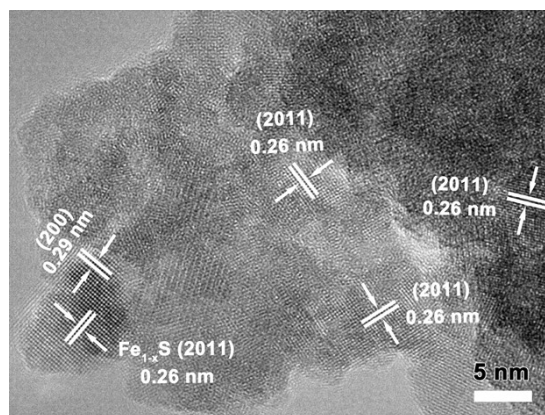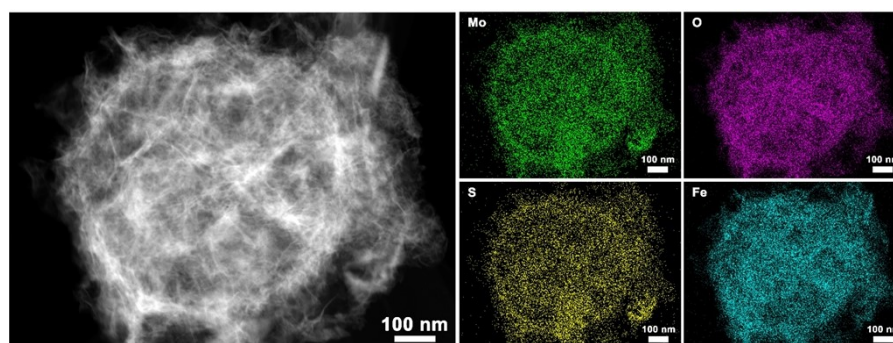
Figure S4. HRTEM of $MoO_x/Fe_{1-x}S/IF$.

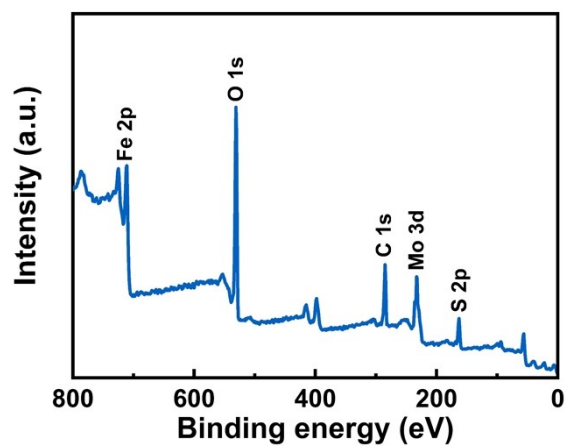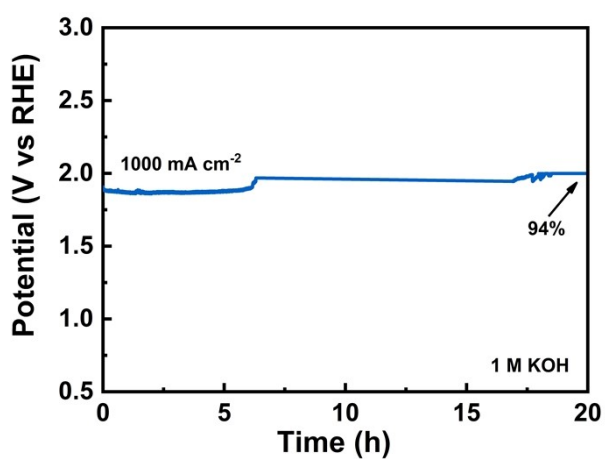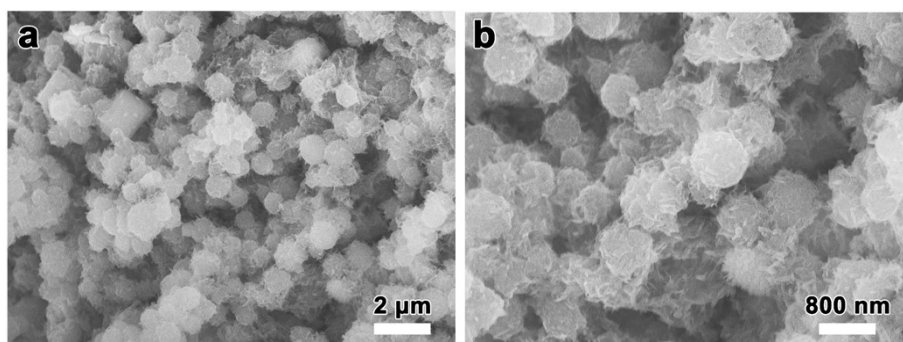**Figure S5.** Corresponding element mapping of $MoO_x/Fe_{1-x}S/IF$.

**Figure S6.** XPS survey spectrum of $MoO_x/Fe_{1-x}S/IF$.
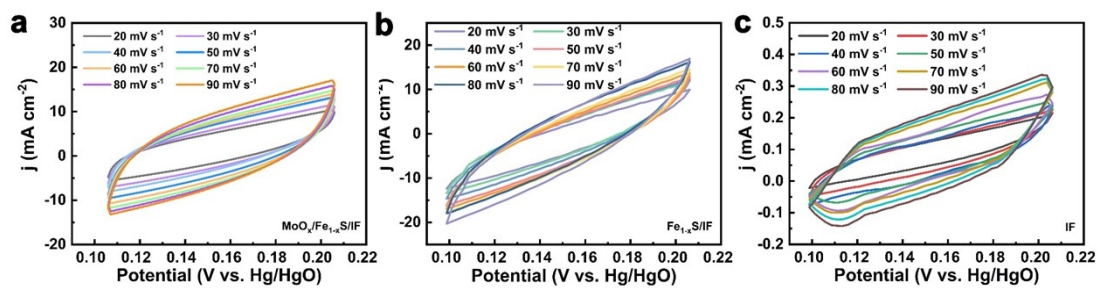
Figure S7. Cyclic voltammogram (CV) curves of (a) $MoO_x/Fe_{1-x}S/IF$, (b) $Fe_{1-x}S/IF$ and (c) IF catalysts electrodes in the region of 0.306 to 1.206 V vs. RHE at different scan rates in 1 M KOH solution.
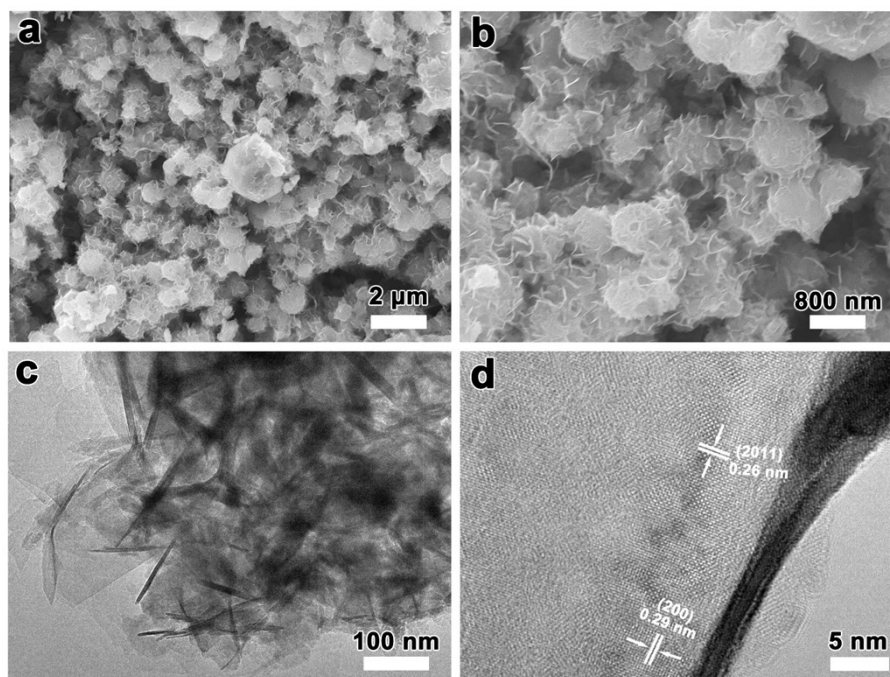

Figure S8. 1000 mA cm^{-2} over 20 h of $MoO_x/Fe_{1-x}S/IF$ in 1 M KOH.

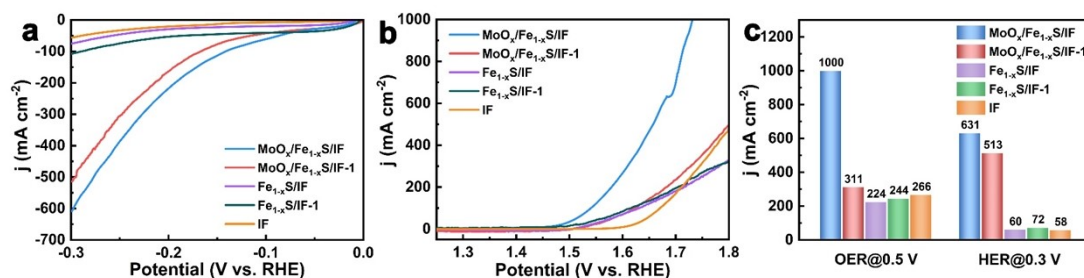**Figure S9.** (a) Low-magnification and (b) high-magnification SEM images of $MoO_x/Fe_{1-x}S/IF$ after long time OER test.
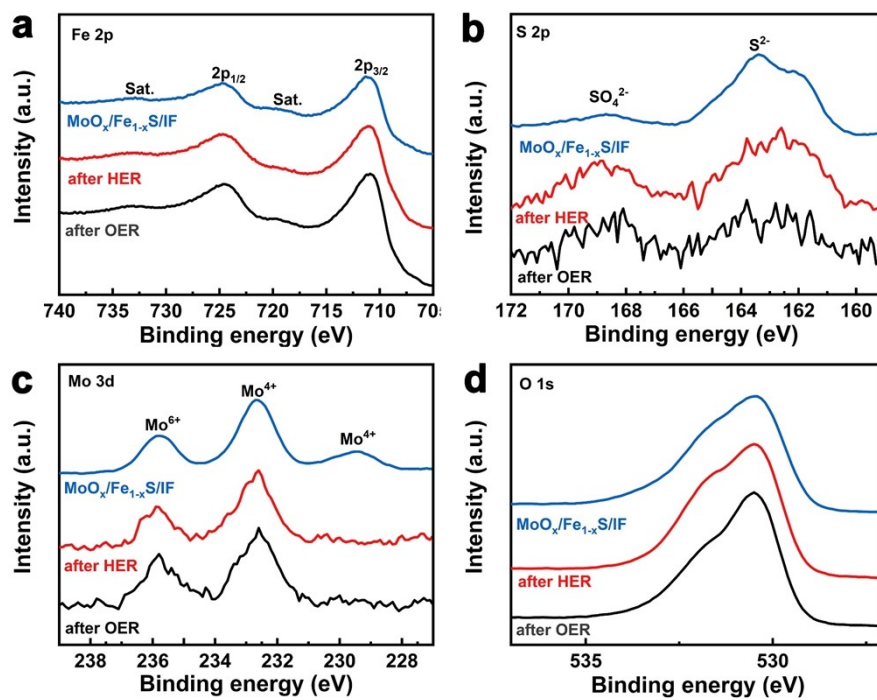
Figure S10. High-resolution XPS spectra of MoO$_x$/Fe$_{1-x}$S/IF before and post OER and HER test. (a) Fe 2p, (b) S 2p, (c) Mo 3d and (d) O 1s.

Figure S11. (a) Low-magnification and (b) high-magnification SEM, (c) TEM, (d) HRTEM images of MoO$_x$/Fe$_{1-x}$S/IF after long time HER test.

Figure S12. (a) 85% iR corrected HER polarization curves, (b) OER polarization curves and (c) Comparison of overpotentials at current densities of OER@0.5 V and HER@0.3 V for $MoO_x/Fe_{1-x}S/IF$, $MoO_x/Fe_{1-x}S/IF-1$, $Fe_{1-x}S/IF$, $Fe_{1-x}S/IF-1$ and IF.

Table S1. The simulated series resistance (R_s), charge transfer resistance (R_{ct}) based on the Nyquist plots (Figure 3c) and ECSA in the presence of $MoO_x/Fe_{1-x}S/IF$, $Fe_{1-x}S/IF$ and IF catalysts.

Catalyst	R_s (Ω cm^2)	R_{ct} (Ω cm^2)	ECSA
$MoO_x/Fe_{1-x}S/IF$	0.28	1.8	153
$Fe_{1-x}S/IF$	0.306	4.44	108
IF	0.4	118	2.9

Table S2. Comparison of electrochemical performance of $MoO_x/Fe_{1-x}S/IF$ in 1 M KOH with other reported highly active bifunctional electrocatalysts.

Catalyst	substrate	HER/ OER	Overpotentials(η) at the corresponding (j)	Stability at j (mA cm^{-2})	Reference
$MoO_x/Fe_{1-x}S/IF$	IF	HER	142 mV@100 mA cm^{-2} 277 mV @500 mA cm^{-2}	100 h	This work
		OER	300 mV @100 mA cm^{-2} 320 mV @500 mA cm^{-2} 500 mV @1000 mA cm^{-2}	17 h	
		OWS	1.56 V@10 mA cm^{-2}	110 h	
$Ni_{0.7}Fe_{0.3}S_2$	NF	HER	155 mV @10 mA cm^{-2}	≈13.8 h	J. Mater. Chem. A, **2017**, 5: 15838-15844
		OER	287 mV @100 mA cm^{-2}	≈13.8 h	
		OWS	1.625 V@10 mA cm^{-2}	≈14 h h	
$(Ni, Fe)S_2@MoS_2$	CFP	HER	130 mV @10 mA cm^{-2}	44 h	Appl. Catal. B: Environ., **2019**, 247: 107-114

		OER	330 mV @100 mA cm^{-2}	44 h	
		OWS	1.56 V@10 mA cm^{-2}	--	
FS-0.9-30	NF	HER	157 mV @10 mA cm^{-2}	1000 cycles	ACS Sustain. Chem. Eng., **2019**, 7: 18015-18026
		OER	255 mV @100 mA cm^{-2}	1000 cycles	
		OWS	1.727 V@10 mA cm^{-2}	≈11 h	
100-NCT-NiCo$_2$S$_4$	PAN	HER	183 mV @10 mA cm^{-2}	12 h	Carbon, **2019**, 145: 521-528
		OER	330 mV @100 mA cm^{-2}	50 h	
		OWS	1.6 V@10 mA cm^{-2}	15 h	
FeP$_x$@Fe	IF	HER	124 mV @10 mA cm^{-2}	24 h	J. Mater. Sci., **2019**, 54: 14872-14883
		OER	274 mV @10 mA cm^{-2}	24 h	
		OWS	1.67 V @10 mA cm^{-2}	5 h	
V-Ni$_3$S$_2$@NiO/NF	NF	HER	239 mV @100 mA cm^{-2}	50 h	ACS Sustain. Chem. Eng., **2020**, 8: 6222-6233
		OER	310 mV @100 mA cm^{-2}	100 h	
		OWS	1.52 V @10 mA cm^{-2}	55 h	
FeS/NiS/NF	NF	HER	202 mV @10 mA cm^{-2}	20 h	Electrochim. Acta, **2020**, 332: 135534
		OER	231 mV @10 mA cm^{-2}	20 h	
		OWS	1.58 V@10 mA cm^{-2}	10 h	
Co-Ni$_3$S$_2$	NF	HER	158 mV @100 mA cm^{-2}	30 h	Small, **2021**, 17: 2102097
		OER	335 mV @100 mA cm^{-2}	25 h	
		OWS	1.54 V@10 mA cm^{-2}	100 h	

Ni$_3$S$_2$@FeNi$_2$S$_4$@NF	NF	HER	143 mV @20 mA cm^{-2}	12 h	J. Colloid Interf. Sci. **2021**, 599: 300–312
		OER	379 mV @100 mA cm^{-2}	--	
		OWS	1.89 V@100 mA cm^{-2}	24 h	
V-Ni$_3$Se$_2$/NF	NF	HER	275 mV @500 mA cm^{-2}	80 h	ACS Sustain. Chem. Eng., **2021**, 9: 12005-12016
		OER	370 mV @500 mA cm^{-2}	80 h	
		OWS	1.56 V@10 mA cm^{-2}	80 h	
NiCoS$_x$@CoCH NAs/NF	NF	HER	199 mV @100 mA cm^{-2} 338 mV @500 mA cm^{-2}	500 h	ACS Appl. Mater. Inter., **2021**, 13: 35647-35656
(Ni$_x$Fe$_y$Co$_{6-x-y}$)Mo6C/NF	NF	OER	336 mV @500 mA cm^{-2}	50 h	Appl. Catal. B: Environ., **2021**, 290: 120049
Ni$_2$P–Ni$_{12}$P$_5$/NF	NF	HER	147 mV @100 mA cm^{-2}	11 h	Small, **2021**, 17(6): 2006770
Ni$_{0.67}$Co$_{0.33}$/Ni$_3$S$_2$@NF	NF	HER	203 mV @100 mA cm^{-2}	11 h	Small, **2022**: 2106904